JOURNAL OF CATALYSIS 98, 491–501 (1986)

Highly Selective Synthesis of Light Olefins from Methanol on a Novel Fe-Silicate

TOMOYUKI INUI, HIROKAZU MATSUDA, OSAMU YAMASE, HIDEO NAGATA, KOICHI FUKUDA, TAKAYO UKAWA, AND AKIRA MIYAMOTO

Department of Hydrocarbon Chemistry, Faculty of Engineering, Kyoto University, Sakyo-ku, Kyoto 606, Japan

Received September 20, 1985; revised December 9, 1985

Methanol to hydrocarbon conversion on a number of metallosilicates having the pentasil pore-opening structure were investigated to develop a highly selective catalyst for the olefin synthesis from methanol. The metallosilicates were prepared by replacing the Al ingredient with various metal salts at the stage of gel formation in a modified preparation method (the rapid crystallization method) of ZSM-5. The catalysts were active for the methanol to hydrocarbon conversion, and the selectivity to lower olefins, gasoline, or aromatics changed greatly with the kind of metal incorporated. As for the conversion to lower olefins, silicates of Fe, Co, and Pt exhibited the best selectivity. Among them, the Fe-silicate was least active for the formation of aromatics—undesirable products caused by a consecutive reaction of olefins. Further investigations were then made for the preparation, characterization, and methanol to hydrocarbon conversion on Fe-silicates. It was found that various amounts of Fe up to 10 wt% as Fe_2O_3 are incorporated in the crystal having pentasil pore-opening structure by the rapid crystallization method. The incorporated Fe was highly dispersed in the crystal and a considerable part of Fe was suggested to be in its framework. The incorporated Fe produced both strong and weak acid sites, and their amounts were controlled by changing Fe content in the catalyst. It was also suggested that a part of the Fe ingredient plays a role as nuclei of crystal growth of the high-silica crystal. The selectivity to C_2–C_4 olefins was greatly increased by the incorporation of Fe in the crystal. The total selectivity to C_2–C_4 olefins was achieved as high as 97.6 C-mol%, and the space-time yield attained 11.9 C-mol/liter · h at 295°C.

INTRODUCTION

Synthesis of light olefins from methanol is one of the most important subjects of investigations in C_1-chemistry (*1–4*). Some zeolites with narrow pores have been found effective for this purpose (*1–16*). ZSM-34 from Mobil Oil Corporation (*5, 6*) and ZKU-4 by Inui *et al.* (*3, 7*) are the most typical examples of catalysts in this category (*1, 17*). The selectivity to ethylene on the former catalyst attained to 50%, and that to C_2–C_4 olefins on the latter catalyst was as high as 81.3%. The most serious problem for these catalysts is the short catalyst life caused by the coke deposition. Although the decrease of the crystalline size and increased uniformity of the crystal caused by the rapid crystallization method (*12–15*) and combination with precious metal component (*16*) have been found useful to increase the catalyst life, further improvements seem necessary for the industrial application of the catalysts. It should also be noted that the coke production on these catalysts is interpreted in terms of the two-dimensional pore structure (*18, 19*).

The ZSM-5 catalyst exhibits a longer catalyst life in the methanol to hydrocarbon conversion because of its pore diameter, inadequate for the formation of fused-ring aromatics and because of the three-dimensional pore structure resistant to the pore blocking (*18, 19*). However, the ZSM-5 catalyst itself is not very selective to the formation of light olefins, because the olefins are further converted to aromatics and paraffins. Modification of ZSM-5 with such compounds as trimethyl phosphine, $Sb(OCH_3)_3$, and $Mg(OCOCH_3)_3$ markedly

0021-9517/86 $3.00

increases the olefin selectivity (*20–25*), probably because the modifier reduces the pore diameter and/or the acid strength. In spite of these advantages the modification of ZSM-5 sometimes greatly decreases the catalytic activity. For this reason, the operation temperature should be considerably raised to attain high-methanol conversion. This in turn increases the coke formation on the modified ZSM-5, providing a subject of further improvements. The strong acid site on the outer surface of ZSM-5 crystal is not effective for the selective reaction of methanol. Although neutralization of the acid site on the outer surface with quinolines has also been found effective to increase the olefin selectivity (*26, 27*), the improvement of the reaction condition does not lead to an essential solution for the industrial application.

Recently, metallosilicates having the pentasil pore opening structure have been expected as catalysts for the olefin synthesis catalyst with high selectivity and long catalyst life (*28–35*). The three-dimensional pore structure would lead to a long catalyst life, and the replacement of the Al ingredient in the ZSM-5 with various kinds of metal salts would greatly modify the nature of active sites, including the acidic property. Furthermore, difference in the metal–oxygen bond length or the coordination of oxygens around the metal would finely control the pore structure inside the zeolitic crystal. Although only a limited number of metallosilicates have been previously prepared, this seems to be due to the lack of the preparation method of metallosilicates. We have previously proposed a new preparation method of ZSM-5—rapid crystallization method (*29*)—which enables us to prepare fine ZSM-5 crystals of uniform size (ca. 1 μm). The rapid crystallization method seems more appropriate than the conventional one for the synthesis of various metallosilicates, since the rate of crystallization may be responsible for the stabilization of a metastable state. The purpose of this study is to prepare various metallosilicates by using the rapid crystallization method and to investigate the catalytic performance of the metallosilicates for the conversion of methanol to hydrocarbons, especially to light olefins. Since the investigation on the methanol conversion on various metallosilicates has revealed that an Fe-silicate is the most effective for the conversion to olefins, further investigations are made for the preparations and characterizations of Fe-silicates to obtain a highly selective olefin synthesis catalyst.

EXPERIMENTAL

1. Preparation of the Metallosilicates

Figure 1 shows the preparation procedure of a metallosilicate by the rapid crystallization method (*29*), while reagents are shown in Table 1. On the basis of a number of experiments on the preparation conditions of ZSM-5, the following improvements were made to prepare uniform and fine zeolitic crystals rapidly: (i) the preparation of supernatant solution was separated from that of gel, which was important for preparing uniform crystals, (ii) the precipitated gel was milled before the hydrothermal treatment, which was essential for obtaining uniform and fine crystals, and (iii) the temperature was programmed under the hydrothermal treatment to minimize the

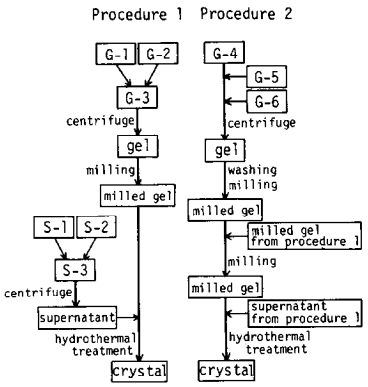

FIG. 1. Procedures for the preparation of a metallosilicate. Procedure 1 is for various metallosilicates including Fe-silicate, while Procedure 2 is for the Fe-silicate with high Fe content (Si/Fe atomic ratio 12).

TABLE 1

Reagents Used for the Preparation of Fe-Silicate

Solution	Si/Fe 3200-25		Si/Fe 12	
G-1	H_2O	60 ml	H_2O	12 ml
	$FeCl_3 \cdot 6H_2O$	x g	$Fe(NO_3)_3 \cdot 9H_2O$	0.04 g
	H_2SO_4	3.38 ml	H_2SO_4	3.38 ml
	TPAB	5.75 g	TPAB	5.75 g
	NaCl	11.95 g	NaCl	11.95 g
G-2		H_2O	45 ml	
		Water glass	69 g	
G-3		H_2O	208 ml	
		NaCl	40.6 g	
		H_2SO_4	1.55 ml	
		TPAB	2.16 g	
		NaOH	2.4 g	
G-4			$Fe(NO_3)_3 \cdot 9H_2O$	27.5 g
G-5			H_2O	136 ml
			Cataloid (SiO_2 30 wt%)	27 g
G-6			25% NH_4OH	15 ml
S-2	H_2O	60 ml	H_2O	70 ml
	$FeCl_3 \cdot 6H_2O$	x g	$Fe(NO_3)_3 \cdot 9H_2O$	0.04 g
	H_2SO_4	3.38 ml	H_2SO_4	3.38 ml
	TPAB	7.53 g	TPAB	7.53 g
S-2		H_2O	45 ml	
		Water glass	69 g	
S-3		H_2O	104 ml	
		NaCl	26.3 g	

Note. TPAB; tetra-propyl ammonium bromide. x; based on Si/Fe charged ratio.

time necessary for the crystallization. As an example, detailed preparation procedures are described below for an Fe-silicate. First, a gel mixture was prepared by adding solution G-1 and solution G-2 into solution G-3 while maintaining a pH within 9–11 at room temperature and vigorously stirring with an ultra disperser. The precipitate was separated from solution by centrifuge. The precipitated gel mixture was milled for a total of 1 h by motor-driven mortar, Yamato-Nitto, UT-21. The milling precipitate and the supernatant of the decant solution from S-1, S-2, and S-3 were mixed together and charged in a 1-liter stainless-steel autoclave. The atmosphere in the autoclave was replaced by N_2 with 3 kg/cm^2 gauge. This was heated from room temperature to 160°C with a constant heating rate, 1.5°C/min, and then up to 210°C with a constant heating rate of 12°C/h. The crystals produced were washed with distilled water by using the centrifugal separator until no Cl ions were detected. The crystals were dried at 120°C for 3 h, and then calcined in an air stream at 540°C for 3.5 h. The calcined crystals were ion-exchanged twice by 1 M NH_4NO_3 solution at 80°C for 1 h. This was washed with distilled water, dried overnight at 100°C, and then heated in air at 540°C for 3.5 h. The charged atomic ratio of Si/metal was 3200 for Ga, Cr, V, Sc, Ge, Mn, La, Al, Ni, Zr, Ti, Co, and Pt, while it varied from 25 to infinity for Fe by changing $FeCl_3$ in solution G-1 and S-1. Since a catalyst of Si/Fe charged ratio 12 could not be prepared by this method (Procedure 1 in Fig. 1), a modified method (Procedure 2 in Fig. 1) was employed to prepare the catalyst of Si/Fe 12; G-4, G-5, and G-6 solutions were used to prepare a milled gel and this was mixed with the one from Pro-

cedure 1. The prepared crystallites were tableted and crushed to 7–15 mesh to provide the reaction.

2. *Characterization of the Catalysts*

BET surface areas of these catalysts were measured by N_2 adsorption with the continuous flow method using the gas chromatograph at liquid N_2 temperature. Helium was used as the carrier gas. The shape and size of the crystals were observed by a Hitachi-Akashi scanning electron microscope (SEM) MSM-102. The acidity of catalysts was measured by using the technique of temperature-programmed desorption (TPD) of NH_3 with a Rigaku thermal analyzer DSC. X-ray diffraction patterns (XRD) of the catalysts were detected by an X-ray analyzer of Rigaku-Denki Geigerflex-2013 with Ni-filtered monochromatic CuKα radiation at an angle (2θ) range of 70 to 7. Chemical compositions of these samples were measured by a Shimadzu atomic absorption spectrophotometer AA-640-01.

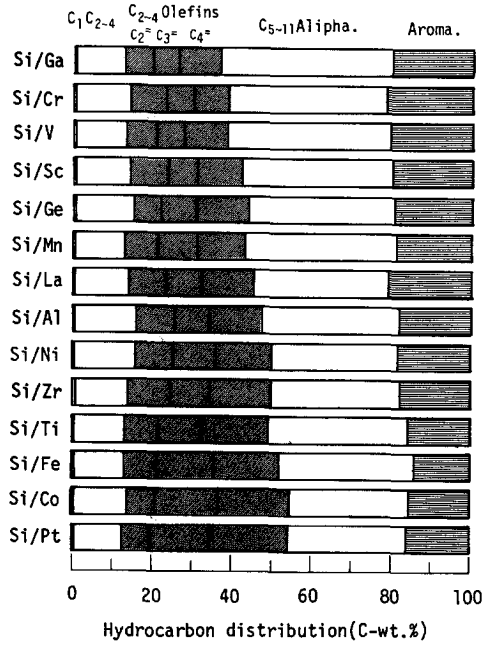

FIG. 2. Hydrocarbon distributions in methanol to hydrocarbon conversion on various metallosilicates with Si/metal charged ratio 3200. Reactant, 20% MeOH and 80% N_2; GHSV, 2000 h^{-1}; temperature, 300°C.

EPMA (electron probe microanalysis) measurements were done with Horiba EMAX 1800E. ESR absorption measurements were made at X-band on a JEOL PE-2X spectrometer at room temperature.

3. *Apparatus and Reaction Method*

The methanol to hydrocarbon conversion reaction was carried out by using a conventional flow apparatus under the following conditions: total pressure, 1 atm; methanol partial pressure, 0.2 atm; balance gas, N_2; catalyst weight, 210 mg (0.3 ml); SV, 2000–8000 h^{-1}; reaction temperature, 295–370°C. The reaction products were analyzed by two FID-type gas chromatographs and a TCD-type one. Columns used were VZ-10 for gaseous hydrocarbons, silicon-OV-101 for gasoline range hydrocarbons, and Porapak T for MeOH, MeOMe, and CO.

RESULTS AND DISCUSSION

1. *Methanol to Hydrocarbon Conversion on Various Metallosilicates with High Si/Metal Ratio*

The X-ray diffraction pattern of any metallosilicate was almost the same as that of H-ZSM-5. This indicates that the metallosilicate also has the pentasil pore-opening structure typical for the ZSM-5 catalyst. The metallosilicate catalyst was active for the methanol to hydrocarbon conversion, and the methanol was completely converted to hydrocarbons under the following condition: reactant, 20% MeOH and 80% N_2; GHSV, 2000 h^{-1}; temperature, 300°C. Figure 2 shows distributions of product hydrocarbons on various metallosilicates under the condition. As shown, the product distribution is greatly changed with the kind of metallosilicate even if the metal content is very small, i.e., Si/metal 3200. Although the results are for the time-on-stream (1 h), no change in activity and selectivity was observed under the present experimental condition. From Fig. 2 the orders of selectivities to olefins, gasoline, and aromatics are respectively determined as follows:

Olefins: Ga ≃ Cr < V < Sc ≃ Ge < Mn < La ≃ Al < Ni < Zr≃ Ti < Fe < Co ≃ Pt;
Gasoline: Ga > V ≃ Cr > Sc > Mn ≃ Ge > La > Al > Ti > Zr ≃ Ni > Fe > Pt ≃ Co;
Aromatics: Cr > La > V ≃ Ga ≃ Sc > Ge > Mn ≃ Ni ≃ Al ≃ Zr > Pt ≃ Ti > Co > Fe.

Fe-silicate, Co-silicate, and Pt-silicate are effective for the conversion of methanol to C_2–C_4 olefins, while Ga-silicate, V-silicate, and Cr-silicate convert methanol to gasoline and aromatics much more selectively than Al-silicate, i.e., H-ZSM-5. The selectivity to aromatics is lowest for Fe-silicate. According to the discussion on the mechanism of methanol conversion to hydrocarbons, low activity for the formation of aromatics is very important for obtaining high selectivity to lower olefins. Thus, further investigations were made for the Fe-silicate to improve the olefin selectivity and to characterize the metallosilicate.

2. *Physical Properties of the Fe-Silicates*

Chemical analysis. Figure 3 shows results of quantitative analysis of Si and Fe ingredients in the synthesized crystals. The observed Fe concentration is almost equal to the charged one, and increases with increasing charged Fe concentration. This indicates that various amounts of Fe can be incorporated in the crystal by changing the charged Fe amount at the stage of gel formation, and almost all of the charged Fe is incorporated in the catalyst. As shown in Fig. 1, the catalyst was prepared through a number of steps. If the interaction of Fe with zeolitic crystal is not strong enough, the Fe may be removed into supernatant solution and/or washing water. Thus, the relationship in Fig. 3 suggests that Fe is strongly held in the crystal.

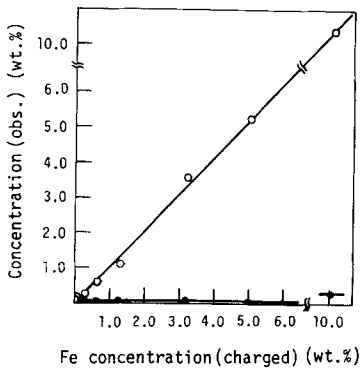

FIG. 3. Relationship between charged and observed Fe concentration for various Fe-silicates. Observed Al concentration; closed circles.

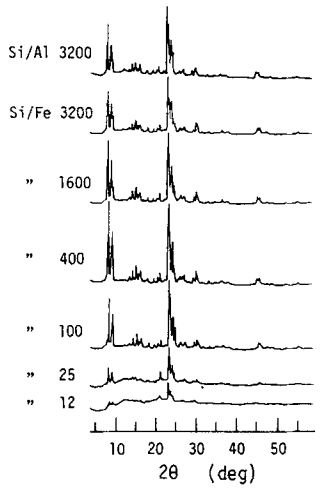

FIG. 4. X-ray diffraction patterns of Fe-silicate catalysts. The number at each pattern stands for Si/Fe charged ratio.

Figure 3 also shows the content of Al in the catalyst. As for the catalyst of Si/Fe charged ratio 3200 or 1600, the amount of Al was larger than that of Fe, while smaller for the catalysts with Si/Fe 400, 200, 100, 40, 25, or 12. The Al in the catalyst may have been brought about by the Al impurity in the water glass.

X-ray diffraction patterns. The X-ray diffraction patterns for the crystals are shown in Fig. 4. All of the patterns of Fe-silicates are similar to that of H-ZSM-5 without the Fe incorporation. This indicates that the Fe-silicate has the pentasil pore-opening structure—the same crystalline structure as ZSM-5. The peak intensities for the catalyst of Si/Fe 12 are weaker than those of higher Si/Fe ratio. This may be due to the decrease in the crystallinity for the former

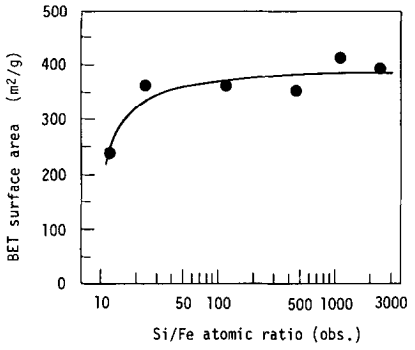

FIG. 5. BET surface area of catalysts.

catalyst. The absence of XRD peaks of iron oxide suggests that the Fe is highly dispersed in the crystal. High dispersion of Fe was also supported by the color of Fe-silicate after calcination (milk-white even for the catalyst with the highest Fe content) which was significantly different from that of iron oxide such as Fe_2O_3.

Specific surface area. BET surface areas for the crystals are shown in Fig. 5. Except for the catalyst of Si/Fe 12, the surface area of Fe-containing crystal was almost as large as that of ZSM-5. This is consistent with the above-mentioned result that the XRD pattern of the Fe-silicate is almost the same as that of ZSM-5. The high BET surface area is also consistent with the high Fe dispersion in the zeolitic crystal. The decrease in the BET surface area for the catalyst of Si/Fe 12 can also be explained in terms of the decrease in the crystallinity of the catalyst.

Morphology. Figure 6 shows SEM photographs of the Fe-free silicate (ZSM-5) and the Fe-silicate of Si/Fe 3200. The addition of Fe greatly affects the morphology of crystal. The crystal of Fe-free silicate is composed of many small crystallites having multisurfaces in plate shapes and it is evidently different from the separated cubics of Fe-silicate of Si/Fe 3200. It is interesting to note that a very small amount of Fe ions (e.g., Si/Fe 3200) can greatly change the shape of crystals, suggesting that a small amount of Fe plays a role as nuclei in the growth of high-silica crystal.

EPMA measurements. According to our preliminary experiments, the measurement of surface Fe concentration by XPS (X-ray photoelectron spectroscopy) was difficult for the catalyst with a high Si/Fe ratio.

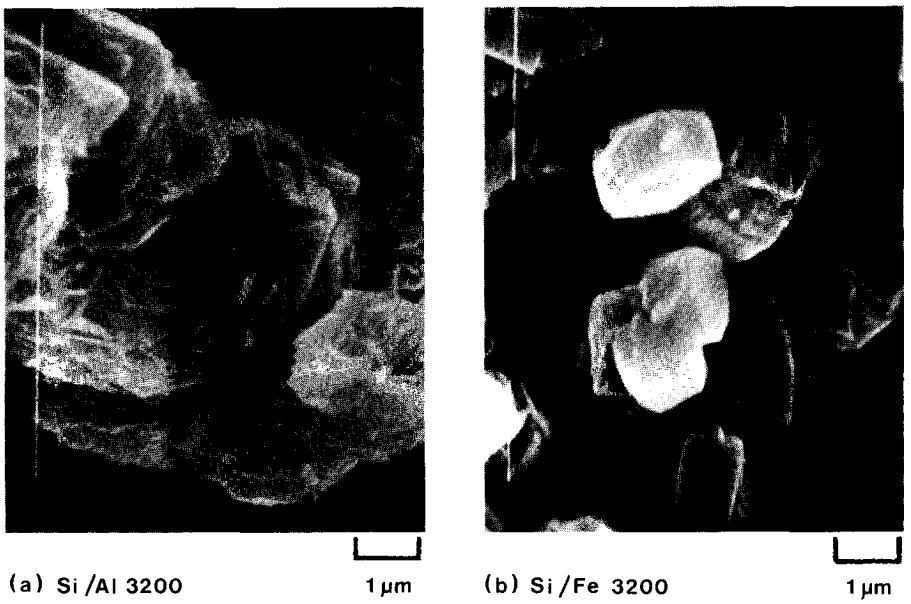

FIG. 6. SEM photographs of the Fe-free silicate (ZSM-5; Si/Al 3200) (a) and Fe-silicate of Si/Fe 3200 (b).

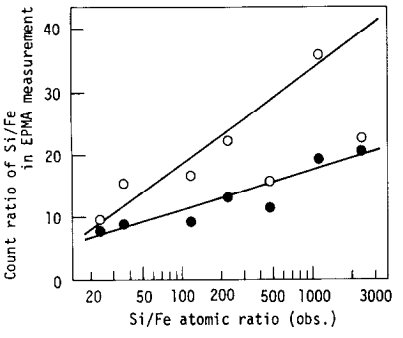

FIG. 7. Si/Fe count ratio in EPMA measurement for nonground (open circles) and ground (closed circles) Fe-silicates.

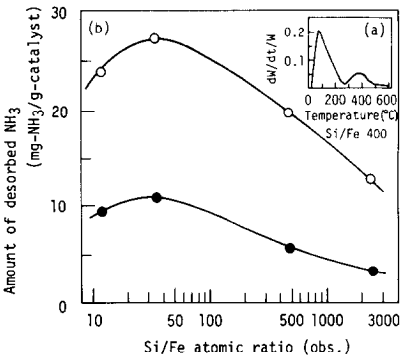

FIG. 9. TPD profile of desorbed NH_3 from the Fe-silicate of Si/Fe 400 (a), and amounts of strong and weak acid sites (b).

Since EPMA was much more sensitive than XPS to a small amount of Fe, the effect of grinding on the Fe concentration was measured by using EPMA to examine the difference in Fe concentration between crystal surface and bulk. As shown in Fig. 7, the Si/Fe count ratio is decreased by the grinding treatment, and the extent of change increases with Si/Fe charged ratio. This indicates that the Fe concentration inside the crystal is higher than that at its surface layers, and supports the above-mentioned idea that Fe plays a role as nuclei of crystal growth in the preparation of high-silica Fe-silicate.

ESR signals of Fe^{3+}. Figure 8 shows ESR signals of Fe^{3+} in the Fe-silicates of various Si/Fe ratios. These signals are similar to those observed by Derouane *et al.* (*36*) for NH_4Y-zeolite, and individual signals are assigned to the following species: (i) Fe^{3+} substitutional ions in the aluminosilicate framework (Fe_S^{3+}) for the signal at $g = 4.4$, (ii) Fe^{3+} ions in exchange sites (Fe_C^{3+}) for the one at $g = 2.0$, and (iii) precipitated Fe^{3+}-containing species on the zeolite structure (Fe_P^{3+}) for the one at $g = 2.1$. In the ESR signal of Fe^{3+} impurities in ammonium-exchanged NaY-zeolite, the intensity of Fe_S^{3+} was much weaker than that of Fe_P^{3+} or Fe_C^{3+}. As shown in Fig. 8, on the other hand, the intensity of Fe_S^{3+} is comparable to that of Fe_P^{3+} or Fe_C^{3+} for the catalysts with high Si/Fe ratios. Since the relative sensitivity of Fe_P^{3+} is much higher than the other species (*36, 37*), a considerable amount of Fe is suggested to be incorporated in the framework of zeolitic crystal for the present Fe-silicate. Further details of the position of Fe ion in the crystal will be investigated by using Mössbauer spectroscopy and solid-state MAS NMR.

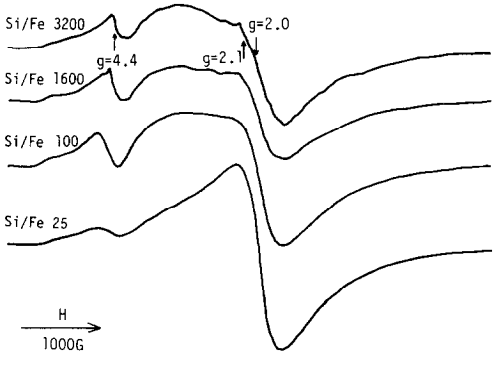

FIG. 8. ESR signals of Fe^{3+} for the Fe-silicates of various Si/Fe charged ratios.

Acidity. Figure 9a shows a TPD profile of desorbed NH_3 from the Fe-silicate of Si/Fe 400 as an example of the TPD profiles from various Fe-silicates. The profile is composed of two peaks, i.e., a high-temperature peak of strong acid sites and a low-temperature peak of weak acid sites (*18, 38–41*). Figure 9b shows the amounts of both peaks for the Fe-silicates of various Si/Fe ratios: the separation of high-temperature and low-temperature peaks were made at 300°C. For both strong and weak acid sites, the amount of the acidic site increases

with decreasing Si/Fe ratio (i.e., with increasing Fe content) in the catalyst except for the catalyst of Si/Fe 12. This indicates that the incorporated Fe ion produces the acidic site and the amount increases with increasing Fe concentration in the catalyst. It is well known that Al in the H-ZSM-5 is responsible for the formation of the acid site, and its number increases with increasing Al content in the catalyst. Judging from the number of Al or Fe ions in the catalyst, the Al may be more important to form the acidic site for the catalyst with high Si/Fe ratio (e.g., Si/Fe 3200), while the Fe is considered to be more important for the catalyst with lower Si/Fe ratio.

Consequently, the Fe^{3+} ion is incorporated in the high-silica crystal having the pentasil pore-opening structure. The ion is in a highly dispersed state and a considerable part of Fe^{3+} is suggested to occupy the framework of the crystal. This can also affect the crystallization process to control the morphology. The incorporated Fe ion plays the acidic site and its amount increases with increasing Fe content in the catalyst. High dispersion of Fe in the crystal was also confirmed by our preliminary experiment about the activity of the incorporated Fe for the syngas ($CO + H_2$) to hydrocarbon conversion. In marked contrast to the behavior of supported iron catalysts, the CO conversion was low and reaction products were mainly CH_4 and CO_2.

3. *Methanol Conversion to Hydrocarbons on Fe-Silicates*

Catalytic performance of Fe-silicates of various Si/Fe ratios. Figure 10a shows hydrocarbon distributions in the methanol conversion on various Fe-silicates, while those on H-ZSM-5 catalysts are shown in Fig. 10b for comparison. The methanol was completely converted to hydrocarbons for the catalysts of Si/Fe above 25. As for the catalyst of Si/Fe 12, the methanol conversion was 78.6%, and 52.3% of the reacted methanol was converted to hydrocarbons while the other part was dimethly ether. As shown, the selectivity for the Fe-silicate is considerably different from that for the H-ZSM-5. As for the Fe-silicate (Fig. 10a, selectivities to C_1–C_4 paraffins and to C_6–C_{11} aromatics are slightly decreased, while that to C_2–C_4 olefins is slightly increased with decreasing Si/Fe ratio in the catalyst. As for the H-ZSM-5 (Fig. 10b), on the other hand, selectivities to C_1–C_4 paraffins and to C_6–C_{11} aromatics are increased, while that to C_2–C_4 olefins is decreased with decreasing Si/Al ratio in the catalyst.

A number of investigations of methanol to hydrocarbon conversion on zeolites suggest the following scheme of the reaction (*1, 42–48*):

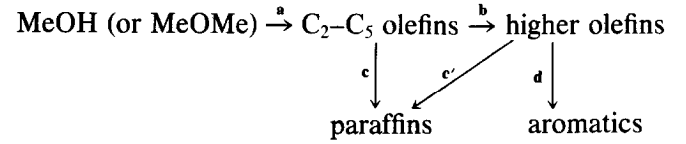

(1)

According to this scheme, methanol or dimethyl ether is first converted to lower olefins (C_2–C_5 olefins) (**a**). The oligomerization (**b**) of the lower olefin leads to the formation of higher olefins ($\geq C_6$ olefins). The hydrogenation of lower and higher olefin forms corresponding to paraffins (**c**, **c'**), and the dehydrogenation and cyclization of higher olefin produces an aromatic molecule (**d**). Although detailed molecular mechanism of individual processes has not yet been clarified, the stoichiometries are described as follows:

Process **b**: $C_nH_{2n} \rightarrow C_mH_{2m}$
$(n = 2, 3, 4, 5), (m \geq 6)$ (2)

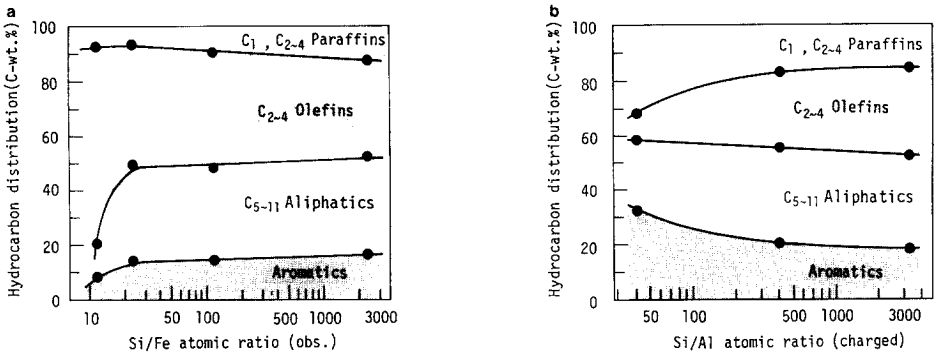

FIG. 10. Hydrocarbon distributions in methanol conversion on Fe-silicates (a) and Al-silicates (H-ZSM-5) (b). Reactant, 20% MeOH and 80% N_2; GHSV, 2000 h^{-1}; temperature, 300°C.

$$\text{Process } \mathbf{c}, \mathbf{c}'\text{: } C_nH_{2n} \xrightarrow{+2H} C_nH_{2n+2} \quad (n \geq 2) \quad (3)$$

$$\text{Process } \mathbf{d}\text{: } C_mH_{2m} \xrightarrow{-xH} C_mH_{2m-x} \quad (m \geq 6). \quad (4)$$

As shown in Eq. (2), neither donation nor abstraction of hydrogen appears in the stoichiometry of the olefin oligomerization (**b**). On the other hand, the donation of hydrogen to olefin molecule is essential for the conversion of olefins to paraffins, (**c**, **c**'), while abstraction of hydrogen is important in the formation of aromatics from olefins (**d**). The lower selectivity to paraffins and aromatics for the Fe-silicate compared with the H-ZSM-5 thus indicates that such an intermolecular hydrogen transfer is suppressed by the incorporation of Fe^{3+} ion in the zeolitic crystal, while the activity for the process without the intermolecular hydrogen transfer is not affected greatly. It should be noted that the lower selectivity to paraffins or aromatics on the Fe-silicate is not due to the lower conversion of MeOH to hydrocarbon. This is because methanol was completely converted to hydrocarbons on all catalysts except for the one of Si/Fe 12, and because our preliminary investigation of the conversion of light olefins indicated a significant difference between the Fe-silicate and the H-ZSM-5 (*33*). In accordance with the above-mentioned idea, the selectivities to aromatics and paraffins on H-ZSM-5 were much higher than those on the Fe-silicate.

Highly selective olefin synthesis. On the basis of the above-mentioned results, we have made trial-and-error experiments to improve the olefin selectivity. Since the presence of Fe salt was suggested to greatly affect the initial step of crystal growth, dilution of Fe in the starting solutions would be effective to optimize the olefin selectivity. Figure 11 shows hydrocarbon distributions in the methanol conversion on the improved Fe-silicate having Si/Fe charged ratio 3200 under the following conditions: reactant, 20% MeOH–80% N_2; SV, 8000 h^{-1}. At 295°C selectivities to ethylene, propylene, and butene are 54.7, 41.5, and 1.4 C-mol%, respectively, and total selectivity to C_2–C_4 olefins attains a high of 97.6 C-mol%.

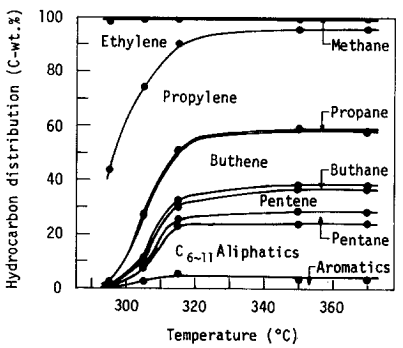

FIG. 11. Methanol conversion on the improved Fe-silicate of Si/Fe 3200. Reactant, 20% MeOH and 80% N_2; GHSV, 8000 h^{-1}.

The space-time-yield (STY) of C_2–C_4 olefins was also increased to 11.9 C-mol/liter · h at 295°C. Also at 350°C the C_2–C_4 olefin selectivity and STY attained 60.8 C-mol% (mainly propylene and butene) and 33.8 C-mol/liter · h, respectively.

In conclusion, an Fe-silicate catalyst is highly effective for the selective conversion of methanol to light olefins. This suggests further applications of metallosilicates to various reactions, providing an interesting subject of future investigations.

ACKNOWLEDGMENT

This work was partially supported by a Grant-in-Aid for Energy Research from the Ministry of Education, Science, and Culture, Japan (No. 60040016).

REFERENCES

1. Chang, C. D., *Catal. Rev.-Sci. Eng.* **25,** 1 (1983).
2. Anthony, R. G., and Singh, B. B., *Hydrocarbon Process.*, Mar. 85 (1981).
3. Inui, T., and Takegami, Y., *Hydrocarbon Process.*, Nov. 117 (1982).
4. Hu, Y. C., *Hydrocarbon Process,* May 88 (1983).
5. Rubin, M. K., Rosinski, E. J., and Plank, J. C., U.S. Pat. 4086186 (1978).
6. Mobil Oil Corp., Japan Kokai 53-58499 (1978).
7. Inui, T., Ishihara, T., Morinaga, N., Takeuchi, G., Matsuda, H., and Takegami, Y., *Ind. Eng. Chem. Prod. Res. Dev.* **22,** 26 (1983).
8. Chang, C. D., Lang, W. H., and Silvestri, A. J., U.S. Pat. 4062905 (1977).
9. Whittam, T. V., and Spencer, M. S., U.K. Pat. Appl. GB2061999A.
10. Lin, F. N., and Anthony, R. G., *Oils Gas J.*, Mar. 92 (1978).
11. Wunder, F. A., and Leupold, E. I., *Angew. Chem. Int. Ed. Engl.* **19,** 126 (1980).
12. Inui, T., Ishihara, T., and Takegami, Y., *J. Chem. Soc. Chem. Commun.*, 936 (1981).
13. Inui, T., Ishihara, T., Morinaga, N., Takeuchi, G., Araki, E., Kanie, T., and Takegami, Y., *Nippon Kagaku Kaishi,* 221 (1982).
14. Inui, T., Morinaga, N., Ishihara, T., Kanie, T., and Takegami, Y., *J. Catal.* **79,** 176 (1983).
15. Inui, T., Morinaga, N., and Takegami, Y., *Appl. Catal.* **8,** 187 (1983).
16. Inui, T., Takeuchi, G., and Takegami, Y., *Appl. Catal.* **4,** 211 (1982).
17. Sheldon, R. A., "Chemicals from Synthesis Gas," p. 78. Reidel, Dordrecht 1983.
18. Dejaifve, P., Aurou, A., Gravelle, P. C., Védrine, J. C., Gabelica, Z., and Derouane, E. G., *J. Catal.* **70,** 123 (1981).
19. Inui, T., *Shokubai (Catalyst)* **25,** 261 (1983).
20. Kaeding, W. W., and Butter, S. A., *J. Catal.* **61,** 158 (1980).
21. Butter, S. A., U.S. Pat. 3979472 (1976).
22. Kaeding, W. W., U.S. Pat. 4049573 (1977).
23. McIntosh, R. J., and Seddon, D., *Appl. Catal.* **6,** 307 (1983).
24. Védrine, J. C., Auroux, A., Dejaifve, P., Ducarme, V., Hoser, H., and Zhou, S., *J. Catal.* **73,** 147 (1982).
25. McIntosh, R. J., and Seddon, D., *Appl. Catal.* **6,** 307 (1983).
26. Kikuchi, E., Hatanaka, S., Hamana, R., and Morita, Y., *J. Japan Petrol. Inst.* **25,** 69 (1982).
27. Inui, T., Fukuda, K., Morinaga, N., and Takegami, Y., *J. Japan Petrol. Inst.* **27,** 188 (1984).
28. Olson, D. H., Haag, W. O., and Lago, R. M., *J. Catal.* **61,** 390 (1980).
29. Inui, T., Yamase, O., Fukuda, K., Itoh, A., Tarumoto, J., Morinaga, N., Hagiwara, T., and Takegami, Y., "Proceedings, 8th International Congress on Catalysis, Berlin, 1984," Vol. 3, p. 569. Dechema, Frankfurt-am-Main, 1984.
30. Ione, K. G., Vostrikova, L. A., Petrova, A. V., and Mastikhin, V. M., "Proceedings, 8th International Congress on Catalysis, Berlin, 1984," Vol. 4, p. 519. Dechema, Frankfurt-am-Main, 1984.
31. Hölderrich, W., Eichhorn, H., Lehnert, R., Marosi, L., Mross, W., Reinke, R., Ruppel, W., and Schlimper, H., "Proceedings, 6th International Conference on Zeolite, Reno, 1984" (D. Olson and A. Bisio, Eds.), p. 545. Butterworths, London, 1984.
32. Ione, K. G., Vostrikova, L. A., Petrova, A. V., and Mastikhin, V. M., "Structure and Reactivity of Modified Zeolites" (P. A. Jacobs *et al.*, Eds.), p. 151. Elsevier, Amsterdam, 1984.
33. Inui, T., *J. Japan Petrol. Inst.* **28,** 279 (1985).
34. Inui, T., Medhanavyn, D., Praserthdam, P., Fukuda, K., Ukawa, T., Sakamoto, A., and Miyamoto, A., *Appl. Catal.*, **18,** 311 (1985).
35. Inui, T., Matsuda, H., and Takegami, Y., "Proceedings, 6th International Conference on Zeolite, Reno, 1984" (D. Olson and A. Bisio, Eds.), p. 316. Butterworths, London, 1984.
36. Derouane, E. G., Mestdagh, M., and Vielvoye, L., *J. Catal.* **33,** 169 (1974).
37. Niwa, M., Yagi, K., and Murakami, Y., *Bull. Chem. Soc. Japan* **54,** 975 (1981).
38. Anderson, J. R., Foger, K., Mole, R., Rajadhyaksha, R. A., and Sanders, J. V., *J. Catal.* **58,** 114 (1979).
39. Topsøe, N. Y., Pedersen, K., and Derouane, E. G. *J. Catal.* **70,** 41 (1981).
40. Hidalgo, C. V., Itoh, H., Hattori, T., Niwa, M., and Murakami, Y., *J. Catal.* **85,** 362 (1984).

41. Inui, T., Suzuki, T., Inoue, M., Murakami, Y., and Takegami, Y., "Structure and Reactivity of Modified Zeolites" (P. A. Jacobs, *et al.*, Eds.), p. 201. Elsevier, Amsterdam, 1984.

42. Chang, C. D., and Silvestri, A. J., *J. Catal.* **47,** 249 (1977).

43. Derouane, E. G., Nagy, J. B., Dejaifve, P., van Hooff, J. H. C., Spekman, B. P., Védrine, J. C., and Naccache, C., *J. Catal.* **53,** 40 (1978).

44. Dessau, R. M., and LaPierre, R. B., *J. Catal.* **78,** 136 (1982).

45. van den Berg, J. P., Wolthuizen, J. P., Clague, A. D. H., Hays, G. R., Huis, R., and van Hooff, J. H. C., *J. Catal.* **80,** 130 (1983).

46. Wu, M. M., and Kaeding, W. W., *J. Catal.* **88,** 478 (1984).

47. Chang, C. D., Chu, C. T. W., and Socha, R. F., *J. Catal.* **86** 289 (1984).

48. Chu, C. T. W., and Chang, C. D., *J. Catal.* **86,** 297 (1984).